

Saw-tooth pattern from flux jumps observed by high resolution M - H curves in MgB_2 thin films

Jae-Yeap Lee,^{1,a)} Hu-Jong Lee,¹ Myung-Hwa Jung,² Sung-Ik Lee,^{2,b)} Eun-Mi Choi,³ and W. N. Kang³

¹Department of Physics, Pohang University of Science and Technology, Pohang 790-784, Republic of Korea

²Department of Physics, National Creative Research Initiative Center for Superconductivity, Sogang University, Seoul 100-611, Republic of Korea

³Department of Physics and BK21 Division, Sungkyunkwan University, Suwon 440-746, Republic of Korea

(Received 23 November 2009; accepted 1 June 2010; published online 6 August 2010)

While flux jumps have been observed in the magnetic hysteresis loops of superconductors, a saw-tooth pattern of the flux jump is known to appear only in a bulk superconductor. But in this study, we were able to observe the saw-tooth pattern in MgB_2 thin film with the careful data acquisition method enhancing the data taking capability and report the details of the distribution of the field interval between jumps B_{fj} , and the size of the flux jump, M_{fj} . The theory based on Bean's model in the adiabatic approach was adapted and it was compared with experimental results. In addition, we observe the cross-over between the saw-tooth pattern and a rounded saw-tooth pattern, as a byproduct. A patterns diagram of the vortex jump was drawn on the H - T plane. © 2010 American Institute of Physics. [doi:10.1063/1.3457674]

I. INTRODUCTION

A magnetic flux jump or avalanche occurs in a superconductor due to a thermomagnetic instability triggered by a positive feedback from the penetration of vortices.¹⁻⁹ Although this flux jump has been observed in a number of superconducting films, it has rarely been observed in bulk superconductors.¹⁰ The shapes of the flux jump of thin films⁹ and the bulk¹⁰ in the magnetic hysteresis (M - H) loops are known to be different. Very large saw-tooth shaped flux jump is observed in a bulk superconductor, but not in a thin film. However, the origin of the flux jump is believed to be the same for both forms of superconductors: a thermo-magnetic instability.²⁻⁹ Therefore, the origin of such difference needs the clear explanation.

Theoretical studies suggest that such instability occurs when the diffusion of vortices is much faster than that of Joule heat generated when vortices penetrate into the superconductors.²⁻⁹ Because of its low thermal conductivity and high critical current density, the magnetic instability of MgB_2 thin film is much pronounced.^{11,12} In bulk MgB_2 , less frequent but very large saw-tooth-shaped flux jump is observed over a wide range of the hysteresis loop.¹⁰ But for MgB_2 thin films, a small flux jump with an irregular shape rather than a saw-tooth shape appears very frequently, and the size of the jump is much smaller than that of the bulk.^{9,13-16}

Previously, the magnetic field intervals between jumps, B_{fj} , in the M - H loop of a bulk superconductor were explained by a theory based on an adiabatic approximation.^{1,3} Although the flux jump in the M - H loop of thin films has been studied widely,^{9,13-16} the saw-tooth pattern of the vortex avalanche has not been observed. This may be due to the low

resolution limit of the measuring equipment. If the detection time of the measurement is fast, it is possible to observe the saw-tooth pattern of the flux jump even in a thin film and we can study the detailed feature of the flux jump behaviors in thin film geometry as investigated at the bulk sample.

In this study, for a very fast measurement time and a very slow sweeping rate with a varying magnetic field, we observed saw-tooth patterns of flux jump for the first time in MgB_2 thin film. Using these results, we can also study about the B_{fj} as a function of the temperature and the applied field. Interestingly, we observed a change from the sharp saw-tooth pattern at low temperatures and low magnetic fields into a rounded saw-tooth pattern at high temperatures and high magnetic fields which is not reported in the bulk sample. Additional information of the height of the flux jump, M_{fj} , was also obtained.

II. EXPERIMENT AND DISCUSSION

The MgB_2 thin film used in this experiment was synthesized by using a two-step method composed of the pulsed laser deposition and the postannealing. The detailed procedures for synthesizing the thin film can be obtained from a previous report.¹⁷ The dimension of thin film was 2.3 mm \times 2.5 mm \times 400 nm.

We measured the magnetic hysteresis loops at applied magnetic field from -5 to 5 T by using a superconducting quantum interference device-vibrating sample magnetometer [(SQUID-VSM): Quantum Design] with a field sweeping rate of 5 Oe/s. This rate is small compared with a few tens of oersted per second in most previous reports.¹³⁻¹⁶ We also took the magnetization signal for every 0.1 s by using the VSM-SQUID, which is one or two orders of magnitude faster than previous measurements made by using a SQUID magnetometer. Due to the slow sweeping rate and the high-speed data-acquisition time, we could obtain at least 1-2

^{a)}Electronic mail: yeaps@postech.ac.kr.

^{b)}Electronic mail: silee77@sogang.ac.kr.

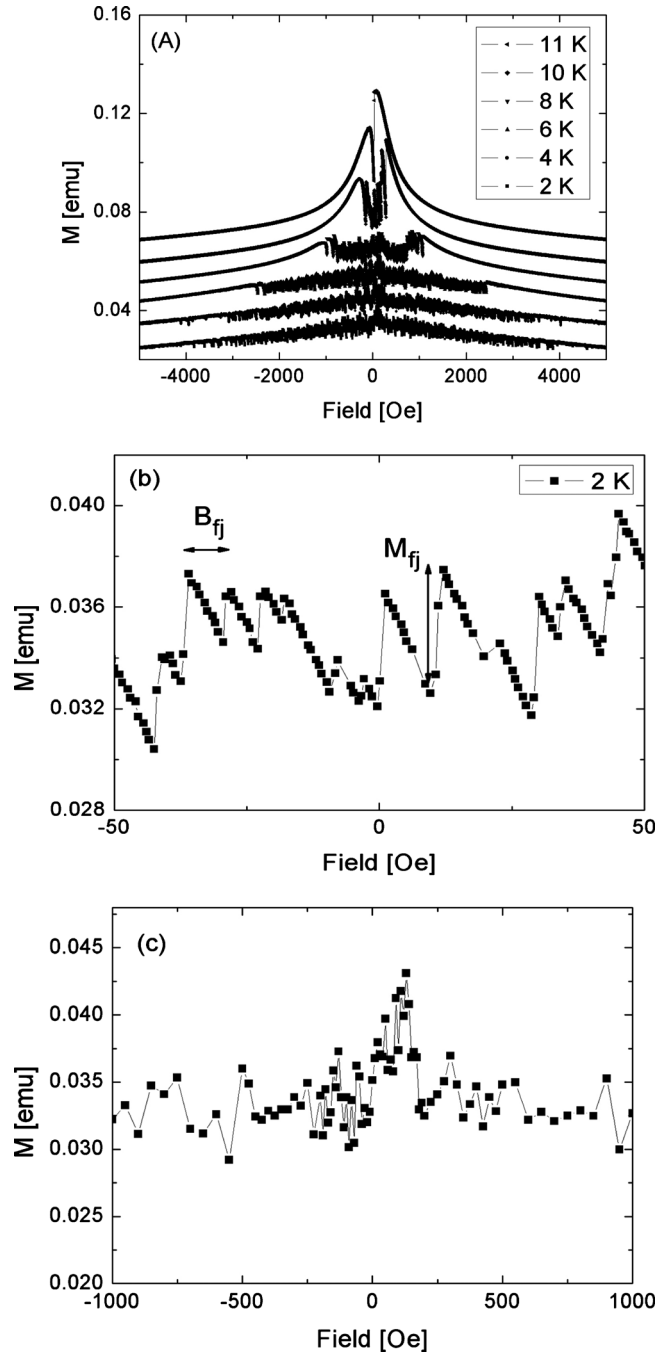


FIG. 1. (a) Remanent parts of magnetic hysteresis loops for temperatures from 2 to 11 K. Results from 4 to 11 K are shifted to upward by 0.01 emu. (b) shows the sharp saw-tooth pattern at 2 K for applied fields between -50 and 50 Oe with sweeping rate of 5 Oe/s and the data-acquisition time interval of 0.1 s. The B_{fj} and the M_{fj} are defined in (b). (c) shows the flux jump in the M - H loop measured by using the conventional SQUID magnetometer at 5 K (Ref. 18). Due to the fewer data points, the real shape of saw-tooth pattern is not captured.

orders of magnitude more data points than in most previous measurements. This allowed the observation of the saw-tooth pattern of flux jump in the M - H curve. The temperature range of our measurements was from 2 to 11 K in 1 or 2 K interval. The superconducting transition temperature was 39 K, which was confirmed by the low-field magnetization measurement.

Figure 1(a) shows the remanent part of the magnetic

hysteresis loop for temperatures from 2 to 11 K at a sweeping rate of 5 Oe/s and the data-acquisition time interval of 0.1 s under the decreasing direction of the magnetic field. Results from 4 to 11 K are shifted to upward by 0.01 emu. The 2 K result lies at the lowest cite and other results are lined to upward with temperatures. Figure 1(b) is an enlarged view of a portion of Fig. 1(a). Figure 1(c) shows an example of the M - H loop, in which the real shape of the flux jump was screened by the fewer data points.⁹⁻¹² As shown in Fig. 1(a), the noise region and the number of flux jump decrease at high temperatures, which is consistent with a previous report.¹⁶ Figure 1(b) shows very clear saw-tooth patterns with a fast data-acquisition time of every 0.1 s. When many vortices jump out from the sample under decreasing of the applied magnetic field, the sudden drop of magnetization which makes vertical step signal in the remanent part appears and there are so many jump behavior compared to the bulk sample. Data points were obtained every 0.8 Oe. The B_{fj} interval of every saw-tooth and the height of the jump, M_{fj} , are indicated in Fig. 1(b).

Figure 2 shows the field dependence of the distribution of the B_{fj} at (a) 2 K, (b) 4 K, and (c) 6 K. The bars in the figure are drawn to guide the eyes. Small B_{fj} stands for more frequent jumps. Figure 2 shows that the B_{fj} is small at low fields, which indicates that the flux penetrates more frequently at low fields. The disappearance of the distribution of B_{fj} at high temperatures indicates the vortex penetration becomes gradual. As shown in Fig. 1(a), flux jump signals appear more densely near the zero magnetic field. An interesting feature in Fig. 2 is that the B_{fj} increases rapidly with increasing magnetic field. For example, the maximum value of B_{fj} at 2 K does not change much at fields below 0.1 T, above which, however, the change is very rapid. This tendency appears in all the graphs of Fig. 2. To explain the field dependence of the B_{fj} , we modify the results in Refs. 3 and 15 based on Bean's model and the adiabatic approach. Because it is known that the thermal conductivity, κ , thickness of the sample, d , and the induced electric field by moving vortices, E also affect to the vortex avalanche,^{15,19} we add above parameters in Eq. (1). J_c is larger and d/w is much smaller than bulk sample,¹⁰ a film show the different flux jump behavior compared to the bulk sample. This formula expresses that as the temperature and the magnetic field go to the threshold value of the vortex avalanche, B_{fj} goes to the divergence which means the stable state.

$$B_{fj}(H, T) = \frac{\mu_0 \kappa J_c}{w |\partial J_c / \partial T| E} \left(\frac{d}{w} \right)^{1/2} \left(\frac{n T_c}{T_{th} - T} \right)^a \left(\frac{H_3}{H_{th} - H} \right)^b, \quad (1)$$

In this relation, $J_c(H, T) = \{2 \exp(-H/H_1) + (1 - T/T_c)[15/(1 + H/H_2)]\} 10^{11}$ A/m².^{15,19} The d and w are the thickness and the width of the sample which can express the demagnetization effect.²⁰ Thermal conductivity, $\kappa = 160(T/T_c)^3$ W/Km and the exponent of the pinning potential, $n = 10(T_c/T - 1)$ are also used in the calculation.¹⁹ T_{th} and H_{th} are the threshold temperature and field of disappearance of the vortex avalanche. The threshold temperature was 13 K (Ref. 16) and the threshold field is varied by the temperature

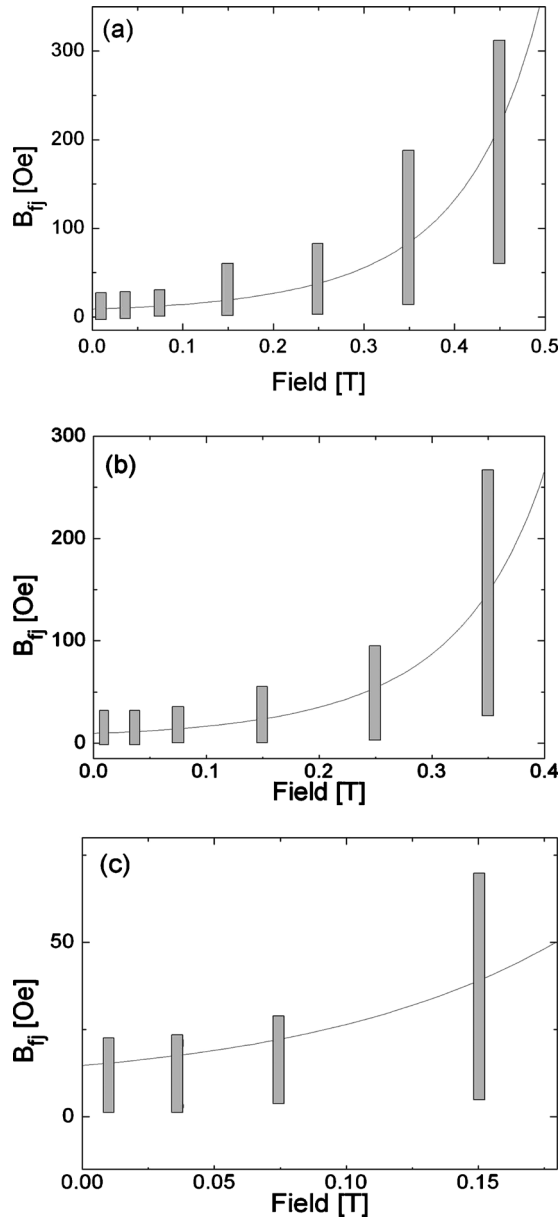


FIG. 2. Distribution of B_{fj} in different field intervals at (a) 2 K, (b) 4 K, and (c) 6 K. The maximum and the minimum of B_{fj} increase with increasing applied field. Bars in figures indicate the distribution of the B_{fj} . Black lines in figures are results from the calculation.

to 0.93, 0.81, and 0.75 T at 2, 4, and 6 K. We also choose these parameters: $H_1=0.028$ T, $H_2=0.1$ T, $H_3=0.001$ T, $E=200$ mV/m, $a=5$, and $b=5$. Using these parameters, we can obtain best results to explain the field dependence of the distribution of B_{fj} indicated in Fig. 2 as black line.

We also investigated the B_{fj} in an enlarged region of the M - H curves, as shown in Fig. 3(a). An abrupt change in the jump pattern is observed. At low magnetic fields, the flux jump has sharp saw-tooth shapes and it changes into a rounded saw-tooth pattern at a certain field value. This change is seen over the entire temperature range of measurements as long as the flux jump occurs. The resulting H - T pattern diagram, which distinguishes the shapes and the stability of vortex pattern, is shown in Fig. 3(b). Curiously, the transition point of the vortex pattern appears at a point around two-thirds of the upper threshold field.

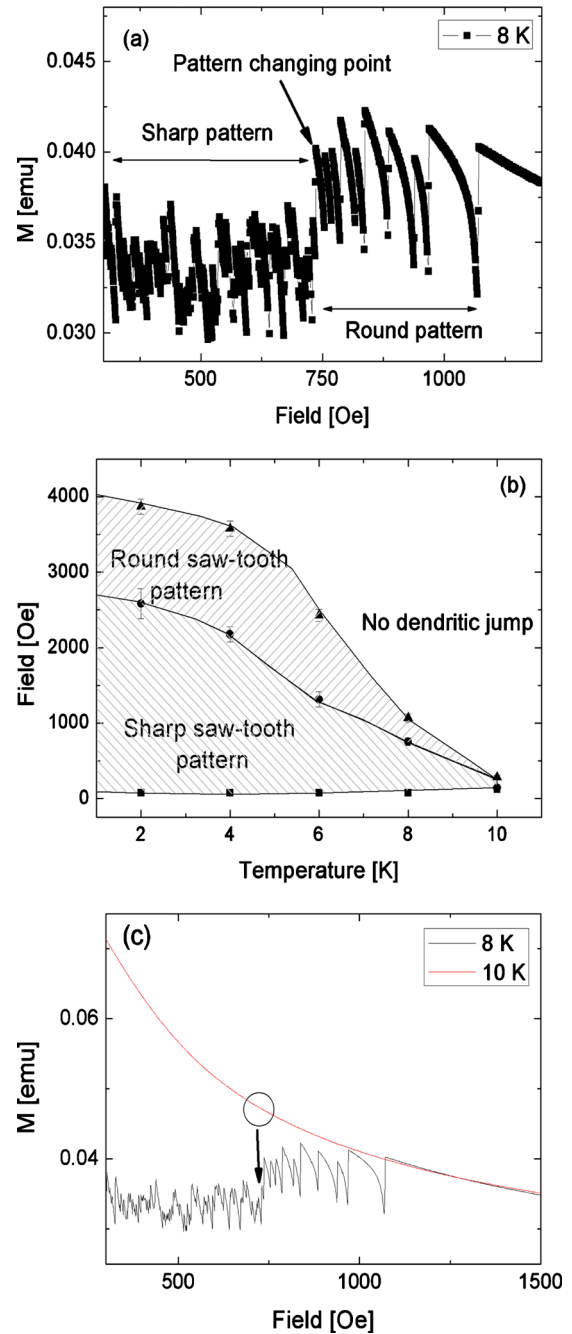


FIG. 3. (Color online) (a) Different jump patterns in the magnetic hysteresis loop at 8 K. The black arrow identifies the transition from a sharp saw-tooth pattern to a rounded one. (b) The H - T pattern diagram illustrates the sharp saw-tooth region, the rounded saw-tooth region, and the no-flux-jump region. (c) The line is M - H curves at 10 K without flux jumps. Result from 10 K is drawn to indicate the hysteresis loop without flux jumps.

Let's discuss the change in saw tooth pattern from sharp saw tooth to the round saw-tooth pattern in Fig. 3. Why the flux jump pattern is changed? Although the flux jump is very complicated phenomenon, we think that the changing of the pattern may be related to the change in the number and size of the flux jump. It is known that the vortex avalanche is affected by the Joule heat expressed by $J \cdot E$. First, vortices penetrate into samples without jump patterns when the shielding current, J , generating Joule heat does not meet the condition for the flux jump and the magnetization value is

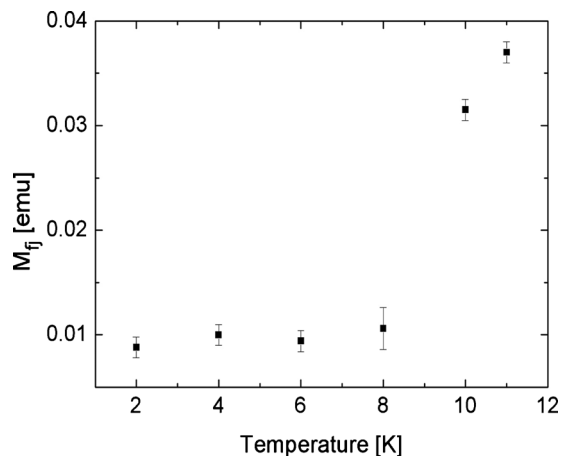


FIG. 4. Temperature dependence of the size of the flux jump M_{fj} .

changed by the applied magnetic field smoothly. But if J exceeds the threshold value inducing the avalanche, the magnetization suddenly drops to the zero point. To make the many jump signals, it is needed that the condition for the flux jump is easily achieved. At the central part of the hysteresis loop, J has larger value than side part and above condition is easily satisfied and it is indicated in M - H curves as a sharp pattern. Round saw tooth pattern which appears in the region having smaller J also can be explained by above foregoing discussion. In this case, the gradient of the flux density between inside and outside of the sample is larger because the applied magnetic field is changed without flux jumps having many vortices. But once the condition for the flux jump is satisfied, more vortices penetrate into the sample than sharp pattern region with larger jump signal making round saw tooth pattern.

Figure 3(c) shows the enlarged hysteresis loops measured at 8 and 10 K. The 10 K M - H loop which does not have flux jump is shifted upward for the effective comparing of M - H result at 8 K with the flux jump. In this figure, we can find that the point of the pattern change at 8 K which is indicated by the circle in the figure is almost same as the point of the rapid change in the M - H curve at 10 K. So, we guess that the one of the possible origin of the pattern change is related to the change in the critical current density. The round saw-tooth pattern of the flux jump is also observed in the MgB_2 bulk case with the lower critical current density. For the bulk superconductor, unstable condition of the flux jump is hardly achievable. However, once flux jump is occurred, the magnetic field interval and the size of the flux jump are large and the shape of the flux jump is round saw-tooth pattern. The common behavior of the round saw-tooth shape flux jump in bulk superconductor and our MgB_2 thin film at the high magnetic field limit indicate that both of the samples are in a similar environment, i.e., round saw-tooth shape occurs at low critical current. This change in the saw-tooth shape is not a phase transition but a cross-over which can be an indicator of how hard the flux instability condition is.

The last point of the discussion is the size of the flux jump, M_{fj} , as defined in Fig. 1(b). The temperature dependence of M_{fj} in Fig. 4 shows that M_{fj} is small and almost

temperature independent below 8 K but it increases sharply above this temperature. As mentioned before, the vortex avalanche is affected by several parameters, such as the critical current density, the specific heat, and the thermal conductivity. As is well known, the combined consequence of all these parameters leads to a more stable vortex configuration at high temperatures with the less-frequent appearance of a vortex avalanche. This is because of the decrease in critical current density and but increase in the specific heat and the thermal conductivity at high temperature. The breakdown condition of the avalanche is not easily achieved in high temperature region. Thus the high magnetic field gradient is induced at the edge of the superconducting film until the flux jump appears. In this case, more vortices penetrate into the sample. Thus, once this happens at high temperatures and high fields, the M_{fj} becomes very large. But above 8 K, the amount of the flux density at the edge of sample increases rapidly and large M_{fj} appears. Since the magnitude of M_{fj} is proportional to the amount of the field accumulation at the edge of the thin films, large M_{fj} can be observed at the high temperature region.

III. SUMMARY

In this study, we investigated the details of the flux jump, B_{fj} while changing the applied magnetic field and the temperature. Three different regions of the flux jump, sharp saw-tooth, round saw-tooth and stable vortex pattern were observed in H - T diagram. For the detailed study of the flux jump, we investigated the distribution of the B_{fj} as a function of the magnetic field and the temperature and it is compared to the theoretical calculation based on Bean's model and the adiabatic approach. The B_{fj} increased with the magnetic field. The size of M_{fj} as a function of the temperature is also measured and discussed. These results are consistent with the thermomagnetic origin of the vortex avalanche.

ACKNOWLEDGMENTS

This work was supported by the Center of Superconductivity of the program of Acceleration Research of Ministry of Science and Technology/Korean Science and Engineering Foundation of Korea and by a special fund from Sogang University.

¹S. L. Wipf, *Phys. Rev.* **161**, 404 (1967).

²K. Chen, S. W. Hsu, T. L. Chen, S. D. Lan, W. H. Lee, and P. T. Wu, *Appl. Phys. Lett.* **56**, 2675 (1990).

³F. L. Barkov, D. V. Shantsev, T. H. Johansen, P. E. Goa, W. N. Kang, H. J. Kim, E. M. Choi, and S. I. Lee, *Phys. Rev. B* **67**, 064513 (2003).

⁴I. S. Aranson, A. Gurevich, M. S. Welling, R. J. Wijngaarden, V. K. Vlasko-Vlasov, V. M. Vinokur, and U. Welp, *Phys. Rev. Lett.* **94**, 037002 (2005).

⁵P. Leiderer, J. Boneberg, P. Brüll, V. Bujok, and S. Herminghaus, *Phys. Rev. Lett.* **71**, 2646 (1993).

⁶D. V. Shantsev, A. V. Bovyl, Y. M. Galperin, T. H. Johansen, and S. I. Lee, *Phys. Rev. B* **72**, 024541 (2005).

⁷D. V. Denisov, A. L. Rakhmanov, D. V. Shantsev, Y. M. Galperin, and T. H. Johansen, *Phys. Rev. B* **73**, 014512 (2006).

⁸A. L. Rakhmanov, D. V. Shantsev, Y. M. Galperin, and T. H. Johansen, *Phys. Rev. B* **70**, 224502 (2004).

⁹Z. W. Zhao, S. L. Li, Y. M. Ni, H. P. Yang, Z. Y. Liu, H. H. Wen, W. N. Kang, H. J. Kim, E. M. Choi, and S. I. Lee, *Phys. Rev. B* **65**, 064512 (2002).

- ¹⁰V. Chabaneko, R. Puzniak, A. Nabialek, S. Vasiliev, V. Rusakov, L. Huang, R. Szymczak, H. Szymczak, J. Jun, J. Karpinski, and V. Finkel, *J. Low Temp. Phys.* **130**, 175 (2003).
- ¹¹H.-J. Kim, W. N. Kang, E.-M. Choi, M.-S. Kim, K. H. Kim, and S.-I. Lee, *Phys. Rev. Lett.* **87**, 087002 (2001).
- ¹²C. Wälti, E. Felder, C. Degen, G. Wigger, R. Monnier, B. Delley, and H. R. Ott, *Phys. Rev. B* **64**, 172515 (2001).
- ¹³E.-M. Choi, H.-S. Lee, H.-J. Kim, S.-I. Lee, H.-J. Kim, and W. N. Kang, *Appl. Phys. Lett.* **84**, 82 (2004).
- ¹⁴E.-M. Choi, H.-S. Lee, H. J. Kim, B. Kang, S.-I. Lee, A. A. F. Olsen, D. V. Shantsev, and T. H. Johansen, *Appl. Phys. Lett.* **87**, 152501 (2005).
- ¹⁵E.-M. Choi, H.-S. Lee, J.-Y. Lee, S.-I. Lee, A. A. F. Olsen, V. V. Yurchenko, D. V. Shantsev, T. H. Johansen, H.-J. Kim, and M.-H. Cho, *Appl. Phys. Lett.* **91**, 042507 (2007).
- ¹⁶J.-Y. Lee, E.-M. Choi, H.-S. Lee, M.-H. Cho, A. A. F. Olsen, T. H. Johansen, Y. S. Oh, K. H. Kim, Y.-H. Han, T. H. Sung, and S.-I. Lee, *J. Phys. Soc. Jpn.* **77**, 104717 (2008).
- ¹⁷W. N. Kang, H.-J. Kim, E.-M. Choi, C. U. Jung, and S.-I. Lee, *Science* **292**, 1521 (2001).
- ¹⁸J.-Y. Lee, H.-J. Lee, S.-I. Lee, C. G. Zhuang, Y. Z. Wang, Q. R. Feng, Z. Z. Gan, X. X. Xi, E.-M. Choi, J.-H. Cho, and Y.-H. Jo, *J. Appl. Phys.* **105**, 083904 (2009).
- ¹⁹D. V. Denisov, D. V. Shantsev, Y. M. Galperin, E.-M. Choi, H.-S. Lee, S.-I. Lee, A. V. Bobyl, P. E. Goa, A. A. F. Olsen, and T. H. Johansen, *Phys. Rev. Lett.* **97**, 077002 (2006).
- ²⁰M. Däumling and D. C. Larbalestier, *Phys. Rev. B* **40**, 9350 (1989).